Journal of Sound and Vibration (1997) **200**(4), 379–399

MODELLING OF THE NOISE SPECTRA OF AXIAL FLOW FANS IN A FREE FIELD

S. F. Wu and S. G. Su

Department of Mechanical Engineering, Wayne State University, Detroit, MI 48202, *U.S.A.*

AND

H. S. Shah

CCD-Fan & Shroud Section, Ford Motor Company, Dearborn, MI 48120, *U.S.A.*

(*Received* 18 *January* 1996, *and in final form* 22 *July* 1996)

This paper presents a semi-empirical formula for predicting the noise spectra of axial flow fans in a free field. The basic assumption made in deriving this formula is that sound radiation from an axial flow fan in a free field is primarily due to the fluctuating pressure exerted on the fan blade surface. This fluctuating pressure is correlated to the lift force per unit length acting on the fan blade, and is subsequently approximated by pressure pulses that decay both in space and time. Accordingly, the radiated acoustic pressure is expressed in terms of superposition of contributions from these pressure pulses, and the line spectrum is obtained by taking a Fourier series expansion. To simulate the narrow and broad band sound spectra, a normal distribution-like shape function is designed which divides the frequency into consecutive bands centered at the blade passage frequency and its harmonics. The amplitude of this shape function at the center frequency of each band is unity but decays exponentially. The decay rate decreases with an increase in the number of bands. Thus, at high frequencies the narrow bands merge to form broad band-like spectra. The noise spectra thus obtained are compared with the measured ones from four different types of axial flow fans running under various conditions, and a favorable agreement in each case is obtained.

1. INTRODUCTION

Reduction of cooling fan noise has become an increasingly urgent task in the automotive industries as the requirements for passenger compartment comfort increase and other vehicle components such as the engine, exhaust system, etc., are made quieter. To reduce fan noise in the most cost-effective manner, it is necessary to incorporate the component of noise reduction into the design stage. For this purpose, one must develop an engineering model that will allow design engineers to estimate noise level given characteristic dimensions and working conditions such as speed, required flow rate (CFM value), etc., of an axial flow fan.

The fundamental theory that governs aerodynamic sound radiation was outlined by Lighthill [1] more than four decades ago. Since then extensive studies of sound radiation from axial flow fans or rotors in a free field have been carried out, for example, by Sharland [2], Van Niekerk [3], Filleul [4], Doak and Vaidya [5], Ffowcs Williams and Hawkings [6], Lowson Ollerhead [7], Wright [8, 9], Mugridge [10, 11], Chandrashekhara [12–14], Barry and Moore [15], Hubbard *et al*. [16], Morfey and Tanna [17], Morfey [18–20], Tam [21], Homicz and George [22], Amiet [23, 24], Longhouse [25, 26], Fukano *et al*. [27, 28], George

0022–460X/97/090379 + 21 $25·00/0/sv960705

and Kim [29], Farassat and Succi [30], Greeley and Kerwin [31], Greeley [32], Eversman *et al*. [33], Farassat *et al*. [34], etc. (The above list of references can be extended, with many equally important works included.)

Because of the complexity of this problem, closed-form solutions to sound radiation from axial flow fans or rotors cannot be found. Therefore the majority of previous studies have focused on a particular noise generation mechanism, such as the fluctuating forces exerted on the medium by the blade, vortex shedding from the trailing edge, etc. Typical examples are given by Lowson and Ollerhead [7], Wright [8, 9], and Farassat and Succi [30], who predicted the discrete line spectra of rotors in a free field due to steady and unsteady fluctuating forces and thickness effect. Homicz and George [22] considered unsteady aerodynamics and distributed loading on the rotor surface based on a cross-correlation, and obtained both the discrete frequency and broad band acoustic signatures generated by aerodynamic rotors. However, when Homicz and George's formula was applied to a low speed axial flow fan, both the discrete frequency and broad band noise level were greatly underestimated. Greeley [31] used the strip theory and derived a formula for estimating the broad band sounds due to vortex shedding from the leading and trailing edges of a rotor. Results showed that when the flow field into the rotor section was specified either through experiment or estimation, the calculated broad band sound levels agreed well with the measured ones.

These examples demonstrate that even with the progress made over the past four decades, the problem of predicting the acoustic signatures of an axial flow fan is still not completely solved. In many engineering applications, one must still rely on some empirical formulae [35] to estimate the total sound power level for given characteristics and operating conditions such as the static pressure drop, the CFM value, etc., to optimize the designs of axial flow fans. Oftentimes, the total sound power level is not enough to characterize the noise performance of an axial flow fan. This is because an axial flow fan has both narrow and broad band components, and in general, the narrow band sounds are more annoying than the broad band sounds. Therefore in order to improve the noise performance of an axial flow fan, it is necessary to be able to predict the spectrum, given the fan characteristic parameters.

The objective of the present paper is to present an engineering model for estimating the noise spectrum of an axial flow fan in a free field. Development of this model is based on the assumption that the radiated acoustic pressure from an axial flow fan is primarily due to the fluctuating pressures exerted on the surrounding fluid medium by the fan blades. These fluctuating pressures are correlated to the lift force per unit length acting on the blade surface calculated by the Blasius theorem over a Joukowski airfoil [36], and subsequently approximated by a series of impulses which decay exponentially in both time and space. Once the fluctuating pressures are specified, the noise spectrum can be determined by taking a Fourier series expansion. To simulate the narrow and broad band sounds, a shape function is designed which breaks the frequency into consecutive bands centered at the blade passage frequency and its harmonics. The amplitude of this shape function at the center frequency of each band is unity, but decays exponentially as the frequency deviates from the center frequency. The decay rate decreases with an increase in the number of bands. Thus at high frequencies the narrow bands merge to form broad band-like spectra. To validate this engineering model, the calculated noise spectra are compared with the measured ones from four different types of axial flow fans running under various conditions.

It is emphasized here that the present formula has been developed for an axial flow fan in a free field where the incident flow is axisymmetric as shown schematically in Figure 1. When the fan is installed in an assembly with a shroud, a radiator and a condenser inside

an engine compartment, the incident flow is not only asymmetric, but also turbulent. Therefore the characteristics of resulting noise radiation will be different, and a different formula must be developed to describe the noise spectrum. While the present formula is valid for the simplest flow condition, it nevertheless provides the guidelines for selecting a quiet axial flow fan, which is the first step toward reducing the passenger compartment noise level.

2. THEORETICAL DEVELOPMENT

The mechanisms of sound radiation from rotors have been well documented by Lowson and Ollerhead [7], Wright [8], Hubbard *et al*. [16], Morfey [19], and more recently by Magliozzi *et al*. [37]. Since it is difficult to describe all of these mechanisms mathematically, and impractical to incorporate all of them into a single model, one chooses to focus attention on the one that influences the predominant feature of the noise spectrum of an axial flow fan in a free field, namely, the fluctuating forces exerted on the fluid medium by the fan blade. This approach is justifiable because the authors intention is to develop an engineering model to estimate the most important feature of the noise spectrum, but not to seek an exact description of the acoustic signature from an axial flow fan. With this basic assumption, one can write the radiated acoustic pressure from an axial flow fan in the following way [7, 8]:

$$sp = -\frac{1}{4\pi} \nabla_x \cdot \left[\frac{\vec{F}}{R}\right]_\tau, \tag{1}$$

where sp stands for the radiated acoustic pressure, $\vec{F}$ represents the force exerted on the fluid by the rotating blades, $R = |\vec{x} - \vec{y}|$ is the distance between an observer at $\vec{x}$ and the source described at $\vec{y}$, ∇_x implies a gradient taken with respect to $\vec{x}$-coordinates, and the square bracket $[]_\tau$ indicates that quantities inside are to be evaluated at the retarded time $\tau = t - R/c$.

Equation (1) shows that if $\vec{F}$ is specified, then the radiated acoustic pressure sp is completely determined. The determination of the surface force has been the subject of extensive studies in the past [7–9, 17–20].

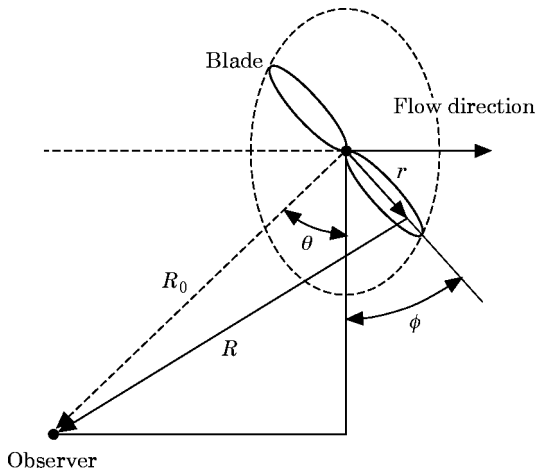

Figure 1. Schematic of an axial flow fan in a free field.

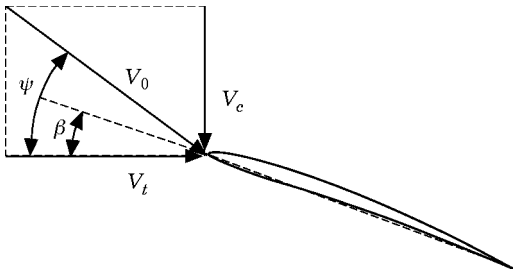

Figure 2. Schematic of the incident flow on an airfoil.

To simplify the problem, one assumes that acoustic radiation is primarily caused by the component of the surface force normal to the blade surface F_n. The contribution from the tangential component of the surface force F_t is negligible compared to that of F_n. Clearly, this assumption will result in a formulation which is valid for an observer near the fan axis region, since F_t acts in the plane of rotation (exerting a torque on the blades), thus having a negligible effect on acoustic radiation in the axial direction. The restriction imposed on the resulting formulation will have a minimum impact on its utility because one is concerned with prediction of noise levels at the position of the driver's ear inside a vehicle, which is around the fan axis region. Hence in calculating the radiated acoustic pressure, one only needs consider F_n, namely, the distribution of the normal component of the surface force F_n.

$$F_n = \iint p\vec{n} \cdot \mathrm{d}\vec{A}, \tag{2}$$

where p is the fluctuating pressure acting on the blade surface area A and $\vec{n}$ is the unit normal vector on the surface.

Since an exact description of the pressure fluctuation p on the blade surfaces for a three dimensional flow cannot be obtained, one chooses to write it in terms of the dynamic pressure multiplied by a constant, an idea borrowed from the description of pressure fluctuations of turbulent flow over an infinite flat plate [2]:

$$p = \xi q, \tag{3}$$

where $q = \rho V^2/2$ is known as the dynamic pressure head, V is the mean flow speed, and ξ is a constant. The commonly accepted value for ξ for an infinite flat plate is between 0·006 [2] and 0·01 [38].

Obviously equation (3) cannot be applied directly to an axial flow fan, because the blade surface area is of a finite extent and its edge effect is non-negligible. In what follows the development of an expression for q is described and it is shown how it is correlated to the lift force per unit length acting on the blade surface.

In aerodynamics, it has been shown that the thrust per unit length acting on a Joukowski airfoil (see Figure 2) can be calculated by using the Blasius theorem [36]

$$F_x - \mathrm{i}F_y = \mathrm{i}\,\frac{\rho}{2} \oint_C \left(\frac{\mathrm{d}w}{\mathrm{d}z}\right)^2 \mathrm{d}z, \tag{4}$$

where w represents the complex potential of the airflow and $\mathrm{d}w/\mathrm{d}z$ is the complex fluid velocity

$$\frac{\mathrm{d}w}{\mathrm{d}z} = \frac{\mathrm{d}w}{\mathrm{d}z_1}\frac{\mathrm{d}z_1}{\mathrm{d}z_2}\frac{\mathrm{d}z_2}{\mathrm{d}z_3}, \tag{5}$$

where z_1, z_2 and z_3 for a Joukowski airfoil are given in reference [36]. With these functions specified, one can calculate a distribution of the mean squared value of velocity $|\,\mathrm{d}w/\mathrm{d}z\,|^2$ along a streamline adjacent to the surface of a Joukowski airfoil (see the solid line in Figure 3). Calculations of $|\,\mathrm{d}w/\mathrm{d}z\,|^2$ suggest that the fluctuating force exerted on a Joukowski airfoil may be approximated by a pulse that decays exponentially along the chord (see the dashed line in Figure 3). This implies that one could use a shape function that decays exponentially along the blade chord to describe the pressure fluctuation p. In the form of equation (3), this is equivalent to writing q as

$$q = q_0\,\mathrm{e}^{-\alpha s}, \tag{6}$$

where q_0 represents the peak amplitude of the pressure pulse, α indicates its decay rate, $s = r\phi$ is the distance along the chord at radius r of the airfoil, and ϕ is the azimuthal angle.

The quantity q_0 in equation (6) can be correlated to the magnitude of the thrust by equating the integral of q over the blade chord to the lift force per unit length F_L,

$$\int_0^{s_0} q\,\mathrm{d}s = \int_0^{s_0} q_0\,\mathrm{e}^{-\alpha s}\,\mathrm{d}s = F_L, \tag{7}$$

where $s_0 = 2\pi r/B$ is the circumference wavelength measured at any radius r, and B is the blade number. Since q_0 is independent of the distance s along the chord, it can be factored out of the integral sign and the result is

$$q_0 = \alpha F_L\,/(1 - \mathrm{e}^{-\alpha s_0}), \tag{8}$$

where F_L is given by [36]

$$F_L = C_L\,\mathscr{C}\rho V_0^2\,/2, \tag{9}$$

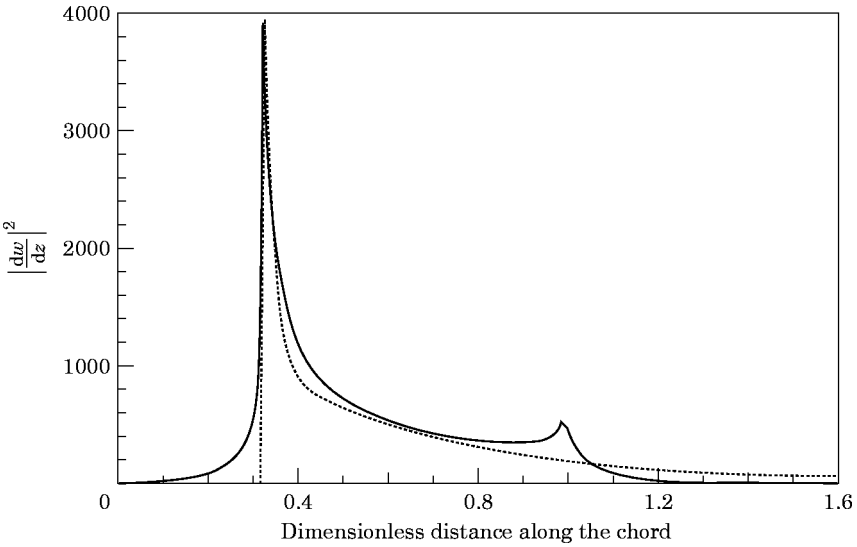

Figure 3. Pressure distribution along the streamline immediately adjacent to the surface of a Joukowski airfoil. Solid line, theory; dashed line, approximation.

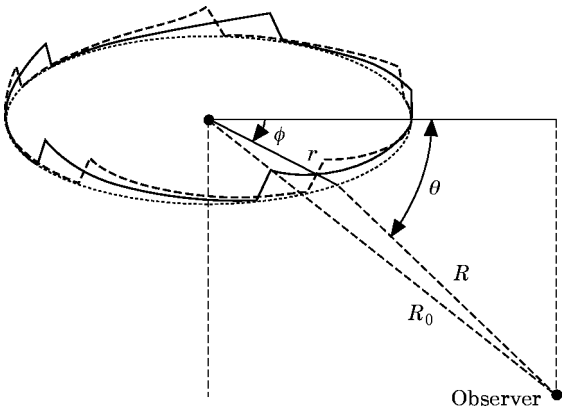

Figure 4. Schematic of the chord-wise distribution of pressure pulses.

where $C_L = a_0 \sin(\psi - \beta)$ is the lift coefficient, ψ, β, and $\mathscr{C}$ represent the angle of the inflow direction, the blade angle, and the chord length at a particular cross section of the blade, respectively, ρ is the density of the fluid medium, V_0 is the magnitude of the incoming mean flow velocity, and a_0 is the lift-curve slope. The commonly accepted value for a_0 is 5·73 [39].

Assume now that the radiated acoustic pressure is expressible as a superposition of pressure pulses emitted from each section of the blade surface. Then for an observer in a fixed co-ordinate system in space (see Figure 4), it is seen that: (1) each pressure pulse has a different emission time as a blade rotates in a circular disk, (2) each pressure pulse decays in time and in azimuth, and (3) each pressure pulse is periodic in time and in azimuth, the period in time being $\tau_0 = f_0^{-1}$ and the period along the azimuth being $s_0 = 2\pi r/B$, where $f_0 = BN/60$ is the blade passage frequency with N being the fan speed in revolution per minute.

With this assumption the shape function q can be rewritten as

$$q = \frac{\alpha F_L}{(1 - e^{-\alpha s_0})} e^{-\alpha r\omega(\tau - l_1 \tau_0)} e^{-\alpha r(\phi - l_2 \phi_0)}, \quad l_{1,2} = 0, 1, \ldots, \text{ to } (B - 1), \tag{10}$$

where ϕ is the azimuthal angle and $\phi_0 = 2\pi/B$.

Physically, the exponential function $e^{-\alpha r\omega(\tau - l_1 \tau_0)}$ in equation (10) represents the decay of the pressure pulse in time at a fixed point on the blade surface, and $e^{-\alpha r(\phi - l_2 \phi_0)}$ represents the decay of the pressure pulse along the azimuth at a fixed time τ.

The concept of describing the radiated acoustic pressure by superimposing contributions of the pressure pulses emitted from the blade surface is not new [9, 34, 37]. The novelty here is the correlation of the shape function of the pressure pulse q to the thrust, or more precisely, to the lift force per unit length F_L. Since only a small fraction of the thrust given by equation (4) is converted to acoustic radiation, it is appropriate to multiply q by a dimensionless coefficient.

In reference [9], Wright shows that the total radiation from the entire source distribution of a rotating blade is expressible as the chord and span spectrum functions, respectively. The chord spectrum function is shown to depend on the chord solidity, namely the ratio of the blade effective chord to the circumference measured at the blade effective radius, which is usually defined as 80% of the blade tip radius. In the present paper, one chooses to define a solidity of the blade surface ξ_b, which is the ratio of the blade surface area to the total blade disk area.

$$\xi_b = B \int_{r_h}^{r_t} \mathscr{C} \cos \beta \, \mathrm{d}r / \pi (r_t^2 - r_h^2), \tag{11}$$

where r_t and r_h represent the tip and hub radii of the blade, respectively.

The reason for selecting ξ_b rather than the chord solidity is to avoid any ambiguity in selecting the blade effective radius. The parameters involved in ξ_b are well defined. One way of defining the coefficient ξ for q then is to set it to be

$$\xi = 1 - \xi_b = \left(\pi (r_t^2 - r_h^2) - B \int_{r_h}^{r_t} \mathscr{C} \cos \beta \, \mathrm{d}r \right) \Big/ \pi (r_t^2 - r_h^2), \tag{12}$$

which represents the ratio of the void area to the total blade disk area. Results show that such a coefficient can yield satisfactory results for fans with straight blades. For a fan with a back-skewed blade, however, this coefficient tends to yield a line spectrum whose amplitude decays at a rate slower than the measured one. Analyses of the experimental data indicate that the decay rate of the line spectrum of a back-skewed fan is proportional to the frequency, as well as to $(1 - \xi_b)$. By trial and error one obtains the following unified empirical expression for ξ:

$$\xi = [0{\cdot}967(1 - \xi_b) - 0{\cdot}294]/[1 - 0{\cdot}0217(1 - \xi_b)\,(f/f_0) \sin(\gamma_h - \gamma)], \tag{13}$$

where f is the frequency of the radiated acoustic pressure, and γ_h and γ represent the blade alignment angles at the hub and at any radius, respectively (see Figure 5). The value of γ is defined as negative for a blade skewed backward and positive for a blade skewed forward. For a straight blade, the alignment angle is identically zero, $\gamma_h = \gamma \equiv 0$. For an inclined but straight blade, the values of γ_h and γ are non-zero but nevertheless are the same. In either case, $\gamma_h - \gamma \equiv 0$, and therefore the denominator of ξ reduces to unity. It is shown in section 5 that the spectra thus obtained by using the coefficient ξ given by equation (13) compare well with the measured ones for both straight and skewed fans.

Substituting equations (10) and (13) into equation (3) thus yields an approximate pressure fluctuation p acting on the fan blade surface. Once p is specified, the normal component of the surface force F_n can be determined by equation (2), and the radiated acoustic pressure can be calculated by equation (1).

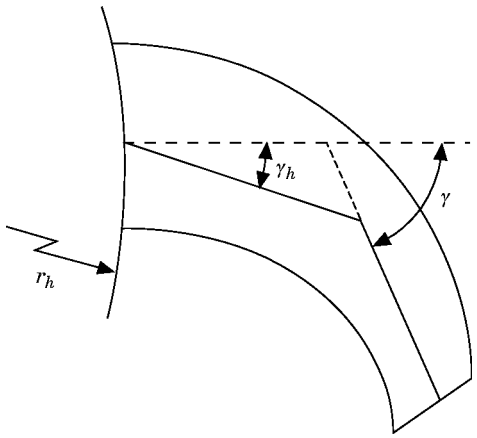

Figure 5. Schematic of the blade alignment angle at hub γ_h and that at any radius γ.

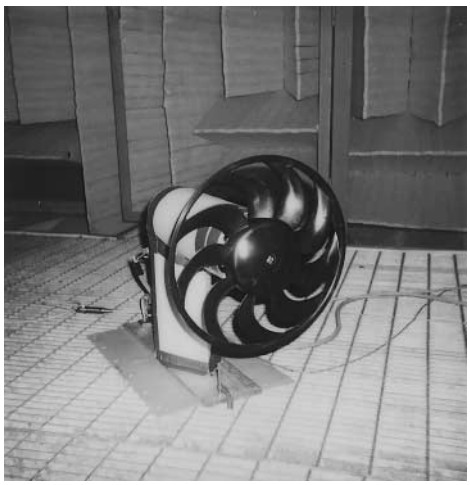

Figure 6. Experimental setup of an axial flow fan inside a fully anechoic chamber.

3. MODELLING THE NOISE SPECTRUM

To obtain the noise spectrum from an axial flow fan, one expands the shape function q given by equation (10) in terms of a Fourier series with respect to both time and azimuth:

$$q = \frac{\alpha F_L}{(1 - \mathrm{e}^{-2\pi\alpha r/B})} \sum_{j=0}^{\infty} a_j \cos(2\pi j B f_0 \tau) \sum_{k=0}^{\infty} b_k \cos(kB\phi), \tag{14}$$

where the coefficients a_j and b_k are given by (Burington [42])

$$a_j = \frac{(2 - \delta_{0j})}{t_0} \int_0^{t_0} \mathrm{e}^{-2\pi f_0 \alpha r \tau} \cos\left(\frac{2\pi j \tau}{\tau_0}\right) \mathrm{d}\tau \approx \frac{(2 - \delta_{0j})B}{2\pi} \frac{(\alpha r)(1 - \mathrm{e}^{-2\pi\alpha r/B})}{(\alpha r)^2 + (jB)^2}, \tag{15a}$$

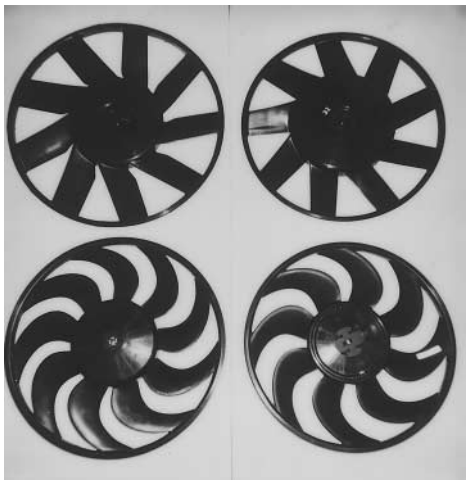

Figure 7. Test fans type A (upper left), type B (upper right), type C (lower left) and type D (lower right).

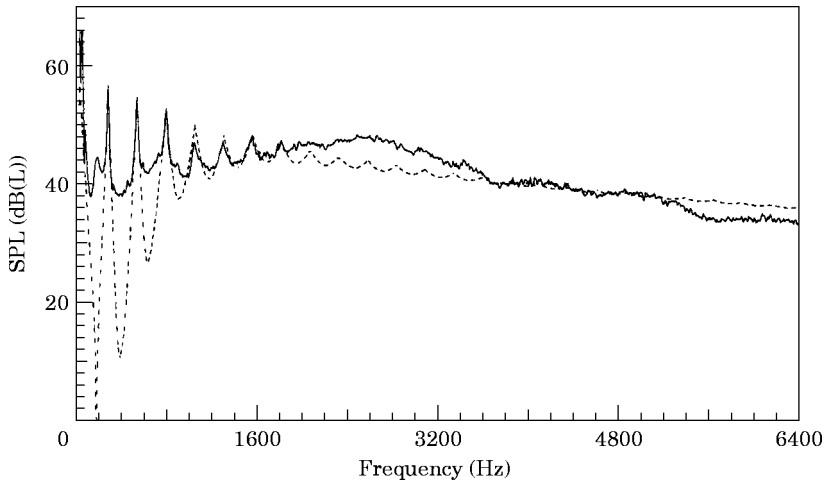

Figure 8. Comparison of the calculated and the measured noise spectra of type A fan at a radial distance $R_0 = 3$ ft along the axis upstream with the fan running at 1706 r.p.m., $\theta = 90^\circ$. Solid line, measurement: dashed line, prediction.

$$b_k = \frac{(2 - \delta_{0k})}{s_0} \int_0^{s_0} e^{-\alpha r \phi} \cos\left(\frac{2\pi k \phi}{\phi_0}\right) d\phi \approx \frac{(2 - \delta_{0k})B}{2\pi} \frac{(\alpha r)\,(1 - e^{-2\pi\alpha r/B})}{(\alpha r)^2 + (kB)^2}, \tag{15b}$$

where δ_{jk} is the Kronecker delta.

Substituting equations (13) and (14) into equation (2) then yields

$$F_n = \iint \frac{\xi \alpha F_L}{(1 - e^{-2\pi\alpha r/B})} \sum_{j=0}^{\infty} a_j \cos(2\pi j B f_0 \tau) \sum_{k=0}^{\infty} b_k \cos(kB\phi) \hat{n} \cdot d\vec{A}. \tag{16}$$

Accordingly, the Fourier series expansion of the radiated acoustic pressure can be written as

$$sp = -\frac{1}{4\pi} \frac{\partial}{\partial n} \left[\frac{F_n}{R}\right]_\tau$$

$$= -\frac{1}{4\pi} \frac{\partial}{\partial n} \iint \left[\frac{\xi \alpha F_L}{R(1 - e^{-2\pi\alpha r/B})} \sum_{j=0}^{\infty} a_j \cos(2\pi_j B f_0 \tau) \sum_{k=0}^{\infty} b_k \cos(kB\phi)\right]_\tau \hat{n} \cdot d\vec{A}. \tag{17}$$

TABLE 1

The peak and total SPL values of type A fan at 3 ft along the axis at 1706 r.p.m.

Peak Number	Frequency (Hz)	Measured SPL (dB(L))	Calculated SPL (dB(L))	Difference (dB(L))
1	256	56·8	56·5	−0·2
2	512	53·4	54·9	+1·5
3	768	52·9	52·2	−0·7
4	1024	47·1	50·0	+2·9
Total SPL	0–6400	71·3 dB(A)	71·3 dB(A)	0·0 dB(A)

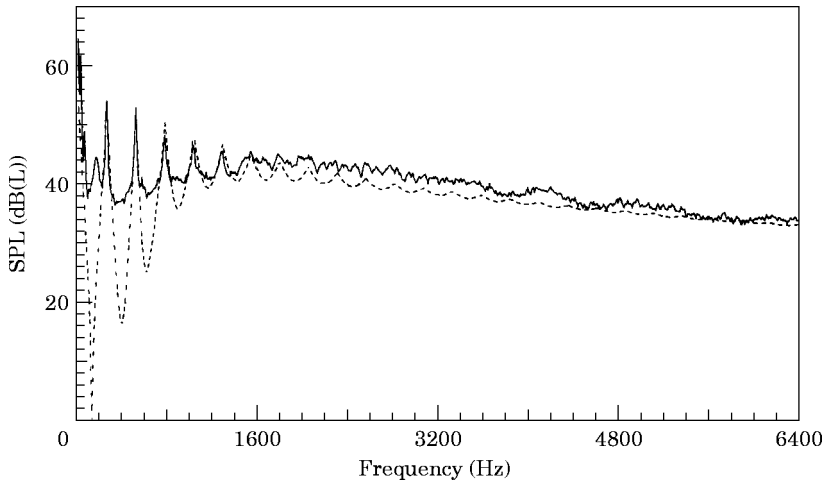

Figure 9. Comparison of the calculated and the measured noise spectra of type A fan at a radial distance $R_0 = 3$ ft and 45° with respect to the fan blade cross-section with the fan running at 1706 r.p.m. Solid line, measurement; dashed line, prediction.

Since F_n is taken to act in the plane normal to the radius vector [8], the derivative $\partial/\partial n$ in equation (17) can be carried out analytically and the result is

$$sp = \iint \frac{R_0\,\xi\alpha F_L\,(\sin\psi\,\cos\theta\,\sin\phi + \cos\psi\,\sin\theta)}{4\pi R^2}\,(1 - \mathrm{e}^{-2\pi\alpha r/B})$$

$$\times \sum_{k=0}^{\infty} b_k \cos(kB\phi)\,\mathrm{Re}\left[\sum_{n=0}^{\infty} a_j \left(\mathrm{i}\,\frac{2\pi jBf_0}{c} - \frac{1}{R}\right)\mathrm{e}^{-\mathrm{i}2\pi jBf_0(t - R/c)}\right]\vec{n}\cdot\mathrm{d}\vec{A}, \tag{18}$$

where R and R_0 are the distances between the source and the center of the blade disk to the receiver, respectively, and θ is the polar angle (see Figure 1).

It can be shown that the integral in equation (18) leads to a series of Bessel functions in the azimuth. To simplify numerical computations, it is assumed that the distance between the measurement point and the blade surface is much larger than the radius of

TABLE 2

The peak and total SPL values of type A fan at 3 ft, 45° and at 1706 r.p.m.

Peak Number	Frequency (Hz)	Measured SPL (dB(L))	Calculated SPL (dB(L))	Difference (dB(L))
1	256	54·8	53·5	−1·3
2	512	52·6	51·9	−0·7
3	768	48·5	49·3	+0·8
4	1024	46·7	47·0	+0·3
Total SPL	0–6400	68·5 dB(A)	68·3 dB(A)	−0·2 dB(A)

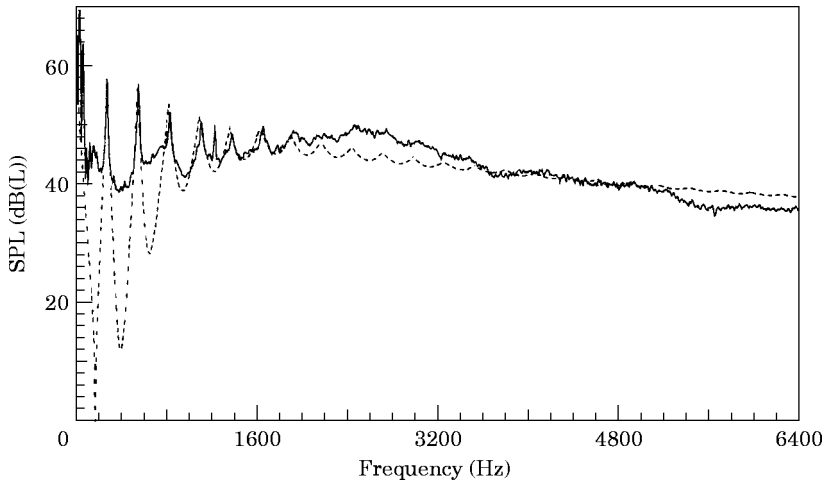

Figure 10. Comparison of the calculated and the measured noise spectra of type A fan at a radial distance $R_0 = 3$ ft along the axis upstream with the fan running at 1978 r.p.m., $\theta = 90^\circ$. Solid line, measurement; dashed line, prediction.

the fan blade section, namely $R \gg r$. Under this condition, $R \approx R_0 - r\cos\phi\cos\phi$. Hence, one can write

$$1/R \approx 1/R_0, \qquad e^{-i2\pi jBf_0(t - R/c)} \cong e^{-i2\pi jBf_0[t - (R_0 - r\cos\phi\cos\phi)/c]}. \tag{19a, b}$$

Substituting equations (19) into equation (18) yields

$$sp = \int_0^{2\pi}\int_{r_h}^{r_t} \frac{\xi\alpha F_L(\sin\psi\cos\theta\sin\phi + \cos\psi\sin\theta)}{4\pi R_0}(1 - e^{-2\pi\alpha r/B})$$

$$\times \sum_{k=0}^{\infty} b_k \cos(kB\phi)\,\mathrm{Re}\left\{\sum_{j=0}^{\infty} a_j\left(i\frac{2\pi jBf_0}{c} - \frac{1}{R_0}\right)e^{-i2\pi jBf_0[t - (R_0 - r\cos\theta\cos\phi)/c]}\right\} r\,dr\,d\phi. \tag{20}$$

Equation (20) can be further simplified if the observation point is close to the fan axis, i.e., $\theta \to 90^\circ$. Under this condition, $\cos\theta \to 0$, $\sin\theta \to 1$, and $R \to \sqrt{R_0^2 + r^2}$. The integration with respect to ϕ in equation (20) can now be carried out separately. Since ϕ varies from

TABLE 3

The peak and total SPL values of type A fan at 3 ft along the axis at 1978 r.p.m.

Peak Number	Frequency (Hz)	Measured SPL (dB(L))	Calculated SPL (dB(L))	Difference (dB(L))
1	296	58·8	60·2	+1·4
2	592	58·0	58·7	+0·7
3	888	51·5	56·0	+4·5
4	1184	51·8	53·8	+2·0
Total SPL	0–6400	74·1 dB(A)	75·6 dB(A)	+1·5 dB(A)

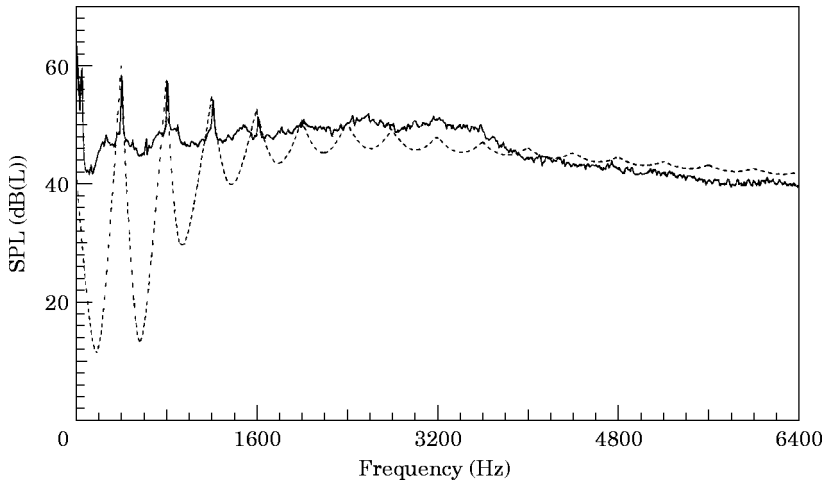

Figure 11. Comparison of the calculated and the measured noise spectra of type B fan at a radial distance $R_0 = 3$ ft along the axis upstream with the fan running at 2684 r.p.m., $\theta = 90^\circ$. Solid line, measurement; dashed line, prediction.

0 to 2π, the integration is non-zero only for the $k = 0$ term. Hence

$$sp = \sum_{j=0}^{\infty} \mathrm{Re}\,(SP_j\, \mathrm{e}^{\mathrm{i}2\pi jBf_0 t}), \tag{21}$$

where SP_j represents the spectrum of the radiated acoustic pressure,

$$SP_j = \int_{r_h}^{r_t} \frac{\xi B^2 F_L\, \alpha r \cos\psi \sin\theta}{8\pi^2 R_0} (1 - \mathrm{e}^{-2\pi\alpha r/B}) \left(\mathrm{i}\frac{2\pi jBf_0}{c} - \frac{1}{R_0}\right)$$

$$\times \frac{(2 - \delta_{0j})\, \mathrm{e}^{\mathrm{i}2\pi jBf_0\sqrt{R_0^2 + r^2}/c}}{(\alpha r)^2 + (jB)^2}\, \mathrm{d}r, \tag{22}$$

where α represents the decay rate of the pressure pulse acting on the blade surface, which is determined via a curve fitting of the experimental data. For the present empirical model, $\alpha = 27{\cdot}4$ seems to yield satisfactory results for all fans under all the test conditions.

Equation (21) thus obtained yields a discrete line spectrum. Experimental data show that for an axial flow fan in a free field, the noise spectrum is composed of the narrow bands centered at the blade passage frequency and its harmonics. These narrow bands are

TABLE 4

The peak and total SPL values of type B fan at 3 ft, along the axis at 2684 r.p.m.

Peak Number	Frequency (Hz)	Measured SPL (dB(L))	Calculated SPL (dB(L))	Difference (dB(L))
1	400	58·0	60·4	+2·4
2	800	57·3	58·0	+0·7
3	1200	54·2	55·4	+1·2
4	1600	50·9	53·3	+2·4
Total SPL	0–6400	75·3 dB(A)	75·9 dB(A)	+0·6 dB(A)

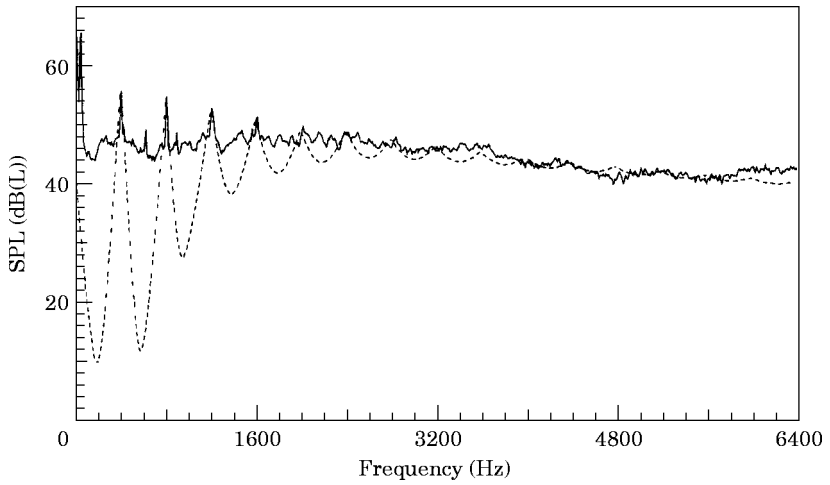

Figure 12. Comparison of the calculated and the measured noise spectra of type B fan at a radial distance $R_0 = 3$ ft and 45° with respect to the fan blade cross section with the fan running at 2684 r.p.m. Solid line, measurement; dashed line, prediction.

predominant in the low frequency regime but decrease with increasing frequency, and gradually blend into broad band sounds at high frequencies. The reasons for the presence of these narrow bands rather than discrete lines are due to random fluctuations in the fan speed as well as in the fluctuating pressures acting on the blade surface. Since it is not possible to derive an explicit formulation to describe these random phenomena, one chooses to devise a normal distribution-like shape function $\mathscr{H}_j$ to simulate the narrow bands:

$$\mathscr{H}_j(f) = \left(1 - \left|\frac{f - jf_0}{f_0}\right|\right) H[f - (j-1)f_0] H[(j+1)f_0 - f]\, \mathrm{e}^{-((f-jf_0)/f_0\sigma_j)^2}, \tag{23}$$

where H is the Heaviside step function

$$H(f - jf_0) = \begin{cases} 0 & \text{if } f < jf_0 \\ 1 & \text{if } f \geqslant jf_0 \end{cases}. \tag{24}$$

These step functions are used to divide the frequency into consecutive bands whose center frequencies coincide with the blade passage frequency and its harmonics. The amplitude of $\mathscr{H}_j$ at the center frequency of each band is unity, but decays exponentially as the frequency deviates from the center frequency. The decay rate of the jth band is determined by σ_j, which is set to be proportional to σ_0 and which increases with the number of bands:

$$\sigma_j = j\sigma_0, \tag{25}$$

where σ_0 is a constant. In this way, the widths of the bands increase with frequency and eventually merge to form a broad band-like spectrum at high frequencies. The larger the value of σ_0, the narrower these bands. Numerical calculations indicate that the noise spectra thus obtained agree well with the measured ones for all the test cases when σ_0 is set at 1/5.

Multiplying the line spectrum SP_j by the shape function given in equation (23) yields the following semi-empirical formula for estimating the noise spectrum of an axial flow

fan in a free field:

$$sp = \sum_{j=0}^{\infty} \mathrm{Re}\,[SP_j\, \mathscr{H}_j(f)\, \mathrm{e}^{-\mathrm{i}2\pi jBf_0 t}], \tag{26}$$

where SP_j can be written, with the substitutions of equations (9) and (13) for F_L and ξ, respectively, as

$$SP_j = \int_{r_h}^{r_t} \frac{\alpha a_0\, r\rho \mathscr{C} B^2 V_0^2\, [0{\cdot}96739(1-\xi_b) - 0{\cdot}2924] \cos\psi \sin\theta \sin(\psi-\beta)}{16\pi^2 R_0\, [1 - 0{\cdot}0217(1-\xi_b)\,(f/f_0)\sin(\gamma_h - \gamma)]}$$

$$\times (1 - \mathrm{e}^{-2\pi\alpha r/B}) \left(\mathrm{i}\frac{2\pi jBf_0}{c} - \frac{1}{R_0}\right) \frac{(2-\delta_{0j})\, \mathrm{e}^{\mathrm{i}2\pi jBf_0\sqrt{R_0^2 + r^2}/c}}{(\alpha r)^2 + (jB)^2}\, \mathrm{d}r, \tag{27}$$

where $V_0^2 = V_t^2 + V_c^2 = 4\pi^2 f^{\,2}(r^2 + \kappa^2)$; here V_t and V_c represent the tangential and axial components of the incident flow velocity (see Figure 2), respectively, and κ is given by

$$\kappa = \mathrm{CFM}/2\pi^2 f(r_t^2 - r_h^2), \tag{28}$$

where the flow rate, i.e., the CFM value is specified as a design parameter of an axial flow fan.

All parameters involved in equation (27) are now completely specified.

Equation (27) indicates that the overall shape of the spectrum is controlled by the decay rate of the pressure pulses α. The solidity of the blade surface ξ_b may affect the shape of the spectrum in the low frequency regime, while the alignment angle γ may affect the spectrum in the high frequency regime. Undoubtedly, there may be other factors that affect the spectrum of an axial flow fan. The parameters shown in equation (27) merely represent the ones that correlate well with present experimental data.

In carrying out the numerical integration in equation (27), the blade is discretized into M strips of equal width Δr in the radial direction. Contributions of sound radiation from each strip are then superimposed. A computer program based on this semi-empirical formula is written in FORTRAN-77.

The input data to this program include: the number of blades B, the speed N and the corresponding CFM value, the hub and tip radii of the fan blade r_h and r_t, the blade alignment angle γ, the number of sections to be discretized over the blade surface M, the chord length $\mathscr{C}$ and the corresponding blade angle β at each discretized section, the density ρ and the speed of sound c of the medium, and the radial distance R_0 and the corresponding polar angle θ of the measurement point with respect to the center of the fan blade cross section.

The output of the program includes the noise spectrum at the measurement point and the A-weighted total sound pressure level (SPL) value in decibels. The entire computation can be completed on a 486 PC within a few seconds of CPU time.

4. EXPERIMENTAL SETUP

Figure 6 shows the test setup for measuring the noise spectrum of an axial flow fan inside a 12 ft × 12 ft × 6·5 ft fully anechoic chamber in the Acoustics, Vibration, and Noise Control Laboratory of Wayne State University. A special stand was designed to hold the fan. The outer surface of this stand was streamlined to reduce the flow resistivity. The fan speed was controlled by a digital DC power supplier and the noise spectra were measured

TABLE 5

The peak and total SPL values of type B fan at 3 ft, 45° and at 2684 r.p.m.

Peak Number	Frequency (Hz)	Measured SPL (dB(L))	Calculated SPL (dB(L))	Difference (dB(L))
1	400	55·7	57·4	+1·7
2	800	54·7	55·0	+0·3
3	1200	52·7	52·4	−0·3
4	1600	51·2	50·3	−0·9
Total SPL	0–6400	73·3 dB(A)	72·9 dB(A)	−0·4 dB(A)

by a B&K Type 4155 condenser microphone. Data acquisition was controlled by a computer, and the signals were analyzed by the STAR-ACOUSTICS software.

5. RESULTS

To validate the semi-empirical formula developed in this paper, we tested four different types of axial flow fans. For proprietary reasons, however, the characteristic dimensions of these fans have been suppressed and only the generic names type A, B, C, and D were used (see Figure 7). For each fan design, the noise spectra were measured at different locations both upstream and downstream under various running conditions. In all cases, favorable agreements between the calculated and measured noise spectra were obtained. In what follows, however, we only present representative comparisons, for the sake of brevity.

5.1. TYPE A FAN

The type A fan is a straight-blade, regular-size axial flow engine cooling fan with nine blades (see Figure 7(a)). Figure 8 demonstrates a comparison of the calculated noise spectrum (dashed line) and the measured one at three ft, along the axis, in the upstream direction with the fan running at around 1706 r.p.m. The overall agreement between the calculated and measured spectra is quite good. In particular, the narrow bands in the low

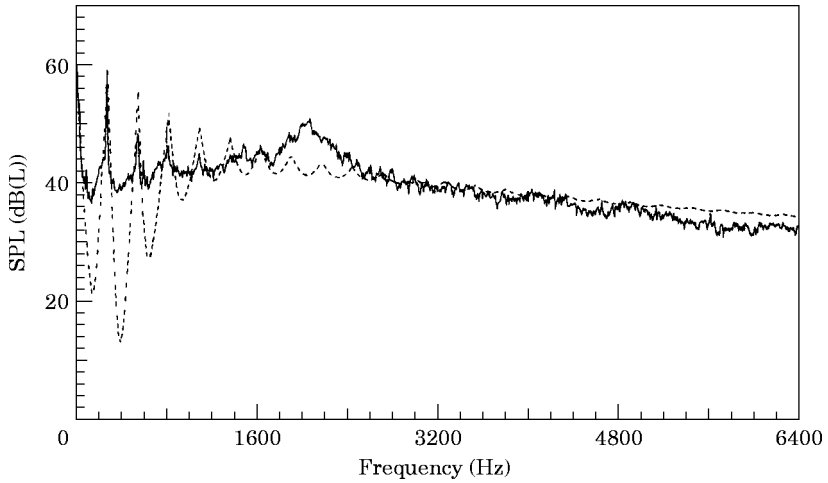

Figure 13. Comparison of the calculated and the measured noise spectra of type C fan at a radial distance $R_0 = 3$ ft along the axis upstream with the fan running at 1811 r.p.m., $\theta = 90°$. Solid line, measurement; dashed line, prediction.

TABLE 6

The peak and total SPL values of type C fan at 3 *ft along the axis at* 1811 *r.p.m.*

Peak Number	Frequency (Hz)	Measured SPL (dB(L))	Calculated SPL (dB(L))	Difference (dB(L))
1	272	59·2	60·8	+1·6
2	554	48·3	55·4	+7·1
3	816	46·3	52·0	+5·7
4	1088	45·0	49·6	+4·6
Total SPL	0–6400	71·3 dB(A)	70·1 dB(A)	−1·2 dB(A)

frequency regime, including the zeroth peak which centers at the shaft frequency, are well captured by the present empirical formula. Moreover, the widths of these narrow bands increase with frequency and eventually merge to form broad band-like spectra. However, some discrepancies between 2000 and 4000 Hz and beyond the 5000 Hz range are noticed. These discrepancies are most likely caused by the leading edge and trailing edge noises [32] that are not accounted for by the present formula.

Table 1 summarizes the SPL values for the first four peaks centered at the blade passage frequency and its harmonics, and the total noise level of 0 to 6400 Hz.

Figure 9 illustrates a comparison of the calculated and measured noise spectra for the same fan at the same distances, but 45° with respect to the fan blade cross-section in the upstream direction. It is interesting to note that the present formula still yields good results at $\theta = 45°$, even though an approximation of a large value of θ ($\theta \to 90°$) in the derivation has been made. The SPL values for the first four peaks and the total noise level in dB(A) are given in Table 2.

A comparison of the calculated and measured noise spectra at $R_0 = 3$ ft upstream on axis with the fan running at 1978 r.p.m. is shown in Figure 10. The corresponding SPL values for the first four peaks and the total noise level are listed in Table 3.

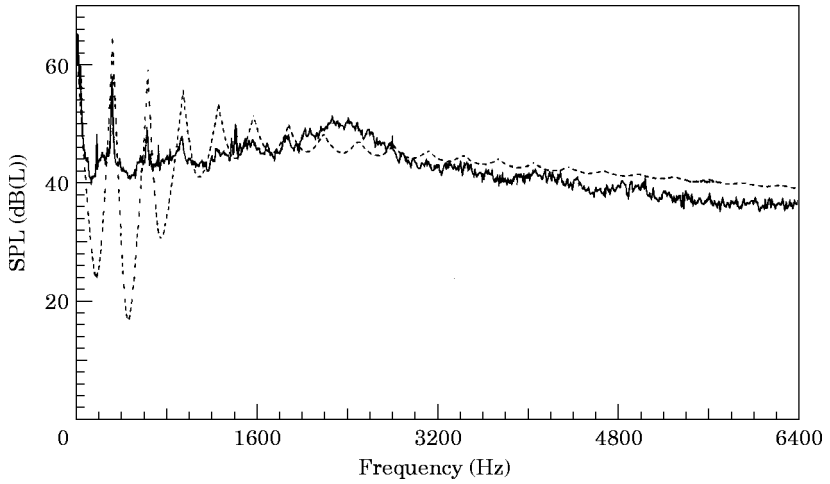

Figure 14. Comparison of the calculated and the measured noise spectra of type C fan at a radial distance $R_0 = 3$ ft along the axis upstream with the fan running at 2026 r.p.m., $\theta = 90°$. Solid line, measurement; dashed line, prediction.

TABLE 7

The peak and total SPL values of type C fan at 3 ft along the axis at 2026 r.p.m.

Peak Number	Frequency (Hz)	Measured SPL (dB(L))	Calculated SPL (dB(L))	Difference (dB(L))
1	312	57·9	63·3	+6·4
2	624	49·3	59·0	+9·7
3	936	47·8	55·6	+7·8
4	1248	45·5	53·1	+7·6
Total SPL	0–6400	73·5 dB(A)	74·2 dB(A)	+0·7 dB(A)

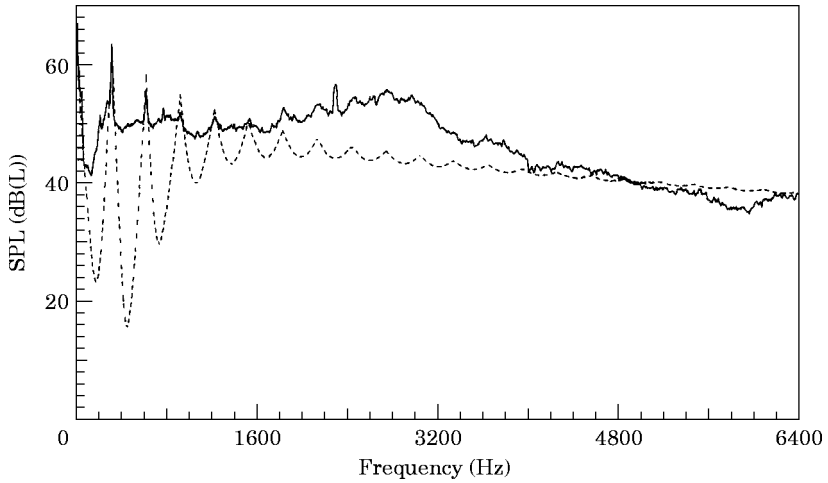

Figure 15. Comparison of the calculated and the measured noise spectra of type D fan at a radial distance $R_0 = 3$ ft along the axis upstream with the fan running at 2252 r.p.m., $\theta = 90°$. Solid line, measurement; dashed line, prediction.

5.2. TYPE B FAN

The type B fan (see Figure 7) also has straight blades, but with almost half the blade inclination angles of the type A fan. Calculations of the incident flow angle based on the given blade inclination angle and camber angle indicate that the type B fan is in the stall region. When this happens, the lift coefficient is greatly reduced. According to Freris [39], the value of C_L may decrease up to 50%. Here $C_L = 0{\cdot}6a_0 \sin(\psi - \beta)$. Namely, a 40% drop in the lift coefficient as compared with the non-stalled situation. Substituting C_L into equation (27) then yields the estimated noise spectrum.

TABLE 8

The peak and total SPL values of type D fan at 3 ft along the axis at 2252 r.p.m.

Peak Number	Frequency (Hz)	Measured SPL (dB(L))	Calculated SPL (dB(L))	Difference (dB(L))
1	304	63·4	63·6	+0·2
2	608	55·5	58·3	+2·8
3	912	51·9	54·9	+3·0
4	1216	51·2	52·4	+1·2
Total SPL	0–6400	77·1 dB(A)	73·4 dB(A)	−3·7 dB(A)

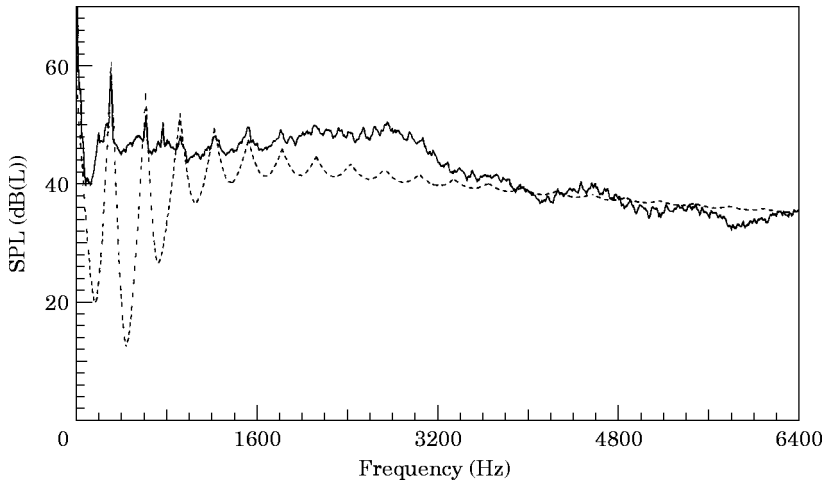

Figure 16. Comparison of the calculated and the measured noise spectra of type D fan at a radial distance $R_0 = 3$ ft and 45° with respect to the fan blade cross-section with the fan running at 2276 r.p.m. Solid line, measurement; dashed line, prediction.

Figure 11 compares the calculated and the measured noise spectra from the type B fan at $R_0 = 3$ ft upstream along the axis with the fan running at 2684 r.p.m. As in the case of the type A fan, the narrow bands in the low frequency regime, including the zeroth band centered at the shaft frequency, are well captured. In particular, in this case a favorable agreement in the mid to high frequency ranges is also obtained. Table 4 summarizes the SPL values for the first four narrow bands and the corresponding total SPL in dB(A).

Figure 12 shows a comparison of the calculated and measured noise spectra for the same fan running at the same speed, but with $R_0 = 3$ ft upstream and $\theta = 45°$ with respect to the fan blade cross-section. Detailed comparisons of the SPL values are listed in Table 5.

5.3. TYPE C FAN

The type C fan is a nine-blade engine cooling fan with a back-swept angle. Using the company supplied fan's characteristic dimensions, geometries, and required working conditions, the resulting noise spectra were estimated. Figure 13 exhibits a comparison of the calculated and measured noise spectra at $R_0 = 3$ ft along the axis upstream with the fan running at 1811 r.p.m. In this case, the SPL values for the second, third, and fourth narrow bands are overestimated, while the noise level for the broad band sounds between 1700 and 2400 Hz range is underestimated. These broad band sounds are caused by the

TABLE 9

The peak and total SPL values of type D fan at 3 ft, 45° and at 2276 r.p.m.

Peak Number	Frequency (Hz)	Measured SPL (dB(L))	Calculated SPL (dB(L))	Difference (dB(L))
1	304	58·9	60·6	+1·7
2	608	51·0	55·2	+4·2
3	912	49·9	51·9	+2·0
4	1216	48·6	49·4	+0·8
Total SPL	0–6400	72·5 dB(A)	70·4 dB(A)	−2·1 dB(A)

trailing edge noises that are not accounted for in the present engineering model. It is interesting to note, however, that despite large discrepancies in the narrow and broad band sounds, the difference in the total SPL value is relatively small (see Table 6). This means that the total radiated acoustic power is more or less captured by the present model.

A similar trend is observed when type C fan is running at other working conditions. Figure 14 demonstrates a comparison of the calculated and measured noise spectrum at the same measurement point but running the designed speed. The discrepancies of the SPL values for the first four narrow bands and the total A-weighted level are summarized in Table 7.

5.4. TYPE D FAN

The type D fan (see Figure 7) is an eight-blade, back swept-type fan with smaller overall dimensions than the type C fan. Using the company supplied data, the resulting noise spectra were calculated. Figure 15 displays a comparison of the calculated spectrum with the measured one at $R = 3$ ft along the axis upstream with the fan running at the designed speed. In this case, the broad band sounds over the 1700 to 4000 Hz range are greatly underestimated. Nevertheless, the SPL values of the first four narrow band sounds are captured (see Table 8).

Figure 16 shows a comparison of the calculated and measured noise spectra at $R = 3$ ft upstream at 45° with respect to the fan blade cross-section. The corresponding SPL values for the first four narrow bands and the A-weighted total level are listed in Table 9.

6. CONCLUDING REMARKS

The semi-empirical formula developed in this paper seems capable of simulating both narrow and broad band sounds of the spectra for the tested axial flow fans in a free field. In particular, it yields more accurate results for a straight blade fan than for a back-swept fan. The reason for that could be due to the fact that a back-swept blade generates more vortex shedding from the trailing edges than a straight blade fan, and the mechanisms of trailing edge noises are not accounted for in this formula. Nevertheless, it can still provide a useful guideline for assessing the noise performance of an axial flow fan in a free field.

ACKNOWLEDGMENTS

The work was supported by Ford Motor Company. The authors would like to thank Mr. D. Nickerson, Supervisor of Heat Exchanger Engineering, Mr. J. J. Firlit, Manager of Heat Exchanger Engineering, Dr. P. T. Thawani, Manager of Climate Control Operation of Ford Motor, and Dr. D. S. Greeley, Manager of Research and Development of the Robert Bosch Corporation for their encouragement and many helpful suggestions during the course of this investigation.

REFERENCES

1. M. J. LIGHTHILL 1952 *Proceeding of the Royal Society of London* **A211**, 564–587. On sound generated aerodynamically. I. General theory.
2. I. J. SHARLAND 1964 *Journal of Sound and Vibration* **1**, 302–322. Sources of noise in axial flow fans.
3. C. G. VAN NIEKERK 1966 *Journal of Sound and Vibration* **3**, 46–56. Noise generation in axial flow fans.
4. N. LE. S. FILLEUL 1966 *Journal of Sound and Vibration* **3**, 147–165. An investigation of axial flow fan noise.

5. P. E. Doak and P. G. Vaidya 1969 *Journal of Sound and Vibration* **9**, 192–196. A note on the relative importance of discrete frequency and broad-band noise generating mechanisms in axial fans.
6. J. E. Ffowcs Williams and D. L. Hawkings 1969 *Journal of Sound and Vibration* **10**, 10–21. Theory relating to the noise of rotating machinery.
7. M. V. Lowson and J. B. Ollerhead 1969 *Journal of Sound and Vibration* **9**, 197–222. A theoretical study of helicopter rotor noise.
8. S. E. Wright 1969 *Journal of Sound and Vibration* **9**, 223–240. Sound radiation from a lifting rotor generated by asymmetric disk loading.
9. S. E. Wright 1971 *Journal of Sound and Vibration* **17**, 437–498. Discrete radiation from rotating periodic sources.
10. B. D. Mugridge 1969 *Journal of Sound and Vibration* **10**, 227–246. The measurement of spinning acoustic modes generated in an axial flow fan.
11. B. D. Mugridge 1976 *Journal of Sound and Vibration* **44**, 349–367. The noise of cooling fans used in heavy automotive vehicles.
12. N. Chandrashekhara 1970 *Journal of Sound and Vibration* **13**, 43–49. Experimental studies of discrete tone noise from an axial flow fan.
13. N. Chandrashekhara 1971 *Journal of Sound and Vibration* **18**, 533–543. Tone radiation from axial flow fans running in turbulent flow.
14. N. Chandrashekhara 1971 *Journal of Sound and Vibration* **19**, 133–146. Sound radiation from inflow turbulence in axial flow fans.
15. B. Barry and C. J. Moore 1971 *Journal of Sound and Vibration* **17**, 207–220. Subsonic fan noise.
16. H. H. Hubbard, D. L. Lansing, and H. L. Runyan 1971 *Journal of Sound and Vibration* **19**, 227–249. A review of rotating blade noise technology.
17. C. L. Morfey and H. K. Tanna 1971 *Journal of Sound and Vibration* **15**, 325–351. Sound radiation from a point force in circular motion.
18. C. L. Morfey 1972 *Journal of Sound and Vibration* **22**, 445–466. The acoustics of axial flow machines.
19. C. L. Morfey 1973 *Journal of Sound and Vibration* **23**, 291–295. The sound field of sources in motion.
20. C. L. Morfey 1973 *Journal of Sound and Vibration* **28**, 587–617. Rotating blades and aerodynamic sound.
21. C. K. W. Tam 1974 *Journal of the Acoustical Society of America* **55**, 1173–1177. Discrete tones of isolated airfoils.
22. G. F. Homicz and A. R. George 1974 *Journal of Sound and Vibration* **36**, 151–177. Broadland and discrete frequency radiation from subsonic rotors.
23. R. K. Amiet 1975 *Journal of Sound and Vibration* **41**, 407–420. Acoustic radiation from an airfoil in a turbulent stream.
24. R. K. Amiet 1976 *Journal of Sound and Vibration* **47**, 387–393. Noise due to turbulent flow past a trailing edge.
25. R. E. Longhouse 1976 *Journal of Sound and Vibration* **48**, 461–474. Noise mechanism separation and design considerations for low tip-speed, axial-flow fans.
26. R. E. Longhouse 1977 *Journal of Sound and Vibration* **53**, 25–46. Vortex shedding noise of low tip speed, axial flow fans.
27. T. Fukano, Y. Kodama and Y. Sendoo 1977 *Journal of Sound and Vibration* **50**, 63–88. Noise generated by low pressure axial flow fans, I: Modelling of the turbulent noise; II: Effects of number of blades, chord length and camber of blade.
28. T. Fukano, Y. Kodama and Y. Takamatsu 1978 *Journal of Sound and Vibration* **56**, 261–277. Noise generated by low pressure axial flow fans, III: Effects of rotational frequency, blade thickness and outer blade profile.
29. A. R. George and Y. N. Kim 1977 *AIAA Journal* **15**, 538–545. High-frequency broadband rotor noise.
30. F. Farassat and G. P. Succi 1980 *Journal of Sound and Vibration* **71**, 399–419. A review of propeller discrete frequency noise prediction technology with emphasis on two current methods for time domain calculations.
31. D. S. Greeley and J. E. Kerwin 1982 *The Society of Naval Architects and Marine Engineers Transactions* **90**, 415–453. Numerical methods for propeller design and analysis in steady flow.
32. D. S. Greeley 1994 *Symposium on Active Control of Vibration and Noise*: *Flow Induced Problems*, ASME International Mechanical Engineering Congress & Exposition, Chicago, Il., U.S.A.
33. W. Eversman, A. V. Parrett, J. S. Preisser and R. J. Silcox 1985 *Transactions of the ASME*

Journal of Vibration, *Acoustics*, *Stress*, *and Reliability in Design* **107**, 216–223. Contributions to the finite element solution of the fan noise radiation problem.
34. F. Farassat, S. L. Padula and M. H. Dunn 1987 *Journal of Sound and Vibration* **119**, 53–79. Advanced turboprop noise prediction based on recent theoretical results.
35. T. Wright 1995 *Noise Control Engineering Journal* **43**, 85–89. The search for simple models to predict fan performance and noise.
36. R. H. F. Pao 1967 *Fluid Mechanics*. Charles E. Merrill Books, See pp. 256–262.
37. B. Magliozzi, D. B. Hanson and R. K. Amiet 1995 in *Aeroacoustics of Flight Vehicles* (Edited by H. H. Hubbard) NASA Reference Publication **1258**, 1–64. Propeller and propfan noise.
38. M. Howe 1991 *Journal of Acoustical Society of America* **90**, 1041–1047. Surface pressures and sound produced by turbulent flow over smooth and rough walls.
39. L. L. Freris 1990 *Wind Energy Conversion Systems*. Prentice Hall, See pp. 68–69.
40. R. S. Burington 1973 *Handbook of Mathematical Tables and Formulas* (Fifth Edition). McGraw-Hill, See pp. 226–230.